Original Paper

Brain, Behavior and Evolution

Brain Behav Evol 1998;51:331–348

Kathryn A. Cortopassi [a]
Edwin R. Lewis [b]

[a] Joint Graduate Group in Bioengineering, Universities of California at Berkeley and San Francisco, Berkeley, Calif.,
[b] Department of Electrical Engineering and Computer Science, University of California at Berkeley, Berkeley, Calif., USA

A Comparison of the Linear Tuning Properties of Two Classes of Axons in the Bullfrog Lagena

Key Words
Bullfrog lagenar macula
Peripheral acoustic sensors
Peripheral equilibrium sensors
Linear amplitude tuning curves
Dynamic order
Inner ear evolution

Abstract
Various vertebrate inner-ear end organs appear to have switched their sensory function between equilibrium sensing and acoustic sensing over the courses of various lines of evolution. It is possible that all that is required to make this transition is to provide an end organ with access to the appropriate stimulus mode and frequency range. If, as we believe, however, the adaptive advantage of an acoustic sensory system lies in its ability to sort the total acoustic input into components that correspond to individual acoustic sources, and the adaptive advantage of an equilibrium sensory system lies in its ability to compute the total orientation and motion of the head without regard to the individual sources contributing to that orientation and motion, then it is easy to argue that the differences between acoustic and equilibrium sensors should be more profound than simply access to the appropriate stimuli. Effective signal-sorting requires high resolution in both time and frequency; to achieve this resolution, a peripheral tuning structure must be one of high dynamic order (i.e., constructed from multiple independent energy storage elements). If the peripheral tuning structure simply converts head acceleration to head displacement, velocity, or jerk (i.e., provides one or two steps of integration or differentiation with respect to time, where one energy storage element per step is required), then high dynamic order is inappropriate. Because the bullfrog lagena possesses both acoustic and equilibrium sensitive regions, it is especially suited for comparing these two sensor types and addressing the question of dynamic order of tuning. In this paper we report observations of the linear tuning properties of bullfrog lagenar primary afferent nerve fibers obtained by stimulating the lagena with random, dorsoventral micromotion over the frequency range from 10 Hz to 1.0 kHz. Tuning curves obtained by reverse correlation analysis and discrete Fourier transformation were used to estimate the dynamic order of each fiber's associated peripheral tuning structure. We found two classes of lagenar afferent axons – those with lowpass amplitude tuning characteristics (44 units) and those with bandpass amplitude tuning characteristics (73 units). Lowpass units were found to originate at the equilibrium region of the macula, and they exhibited low dynamic order – summed low- and high-frequency slopes (absolute values) ranged from 10 dB/decade to 64 dB/decade, implying dynamic orders of less than one to three (the modal value was equal to one). Bandpass units were found to originate at the acoustic region of the macula, and they exhibited higher dynamic order than lowpass units – summed low- and high-frequency slopes (absolute values) ranged from 53 dB/decade to 185 dB/decade, implying dynamic orders of three to nine (the modal value was equal to five). It appears that while lagenar equilibrium and acoustic sensors both possess access to signals in the acoustic frequency range, lagenar acoustic sensors are tuned by means of peripheral structures with markedly greater dynamic order and consequently markedly greater physical complexity. These results suggest that steep-sloped (high-dynamic-order) tuning properties reflect special adaptations in acoustic sensors not found in equilibrium sensors, and that any evolutionary transition between the two sensor types must have involved profound structural changes.

KARGER

Fax + 41 61 306 12 34
E-Mail karger@karger.ch
www.karger.com

This article is also accessible online at:
http://BioMedNet.com/karger

Kathryn A. Cortopassi, PhD, c/o Edwin R. Lewis
Department of Electrical Engineering and Computer Science
University of California at Berkeley
Berkeley, CA 94720 (USA)
Tel. 510-642-6954, Fax 510-643-8426
E-Mail Lewis@EECS.Berkeley.edu

Introduction

The generalized vertebrate inner ear can possess as many as nine end organs; these include the three semicircular canal cristae, the utricular macula, the macula neglecta, the saccular macula, the lagenar macula, the basilar papilla (or cochlea in mammals), and the amphibian papilla. Each of these end organs is involved in one of the two sensory functions (sometimes both) accomplished by vertebrate ears, acoustic sensing and equilibrium sensing. While equivalently named end organs are believed to be homologous across vertebrate taxa, a given end organ can possess quite different sensory function in different taxa. This is true especially for the otolithic and otoconial end organs – the utricle, sacculus and lagena. These end organs appear to have switched their sensory function from equilibrium sensing to acoustic sensing several times over the courses of various lines of vertebrate evolution [Lewis, 1992]. Consider, for example, the saccular macula. The sacculus of the bullfrog has purely acoustic function [Koyama et al.,1982; Lewis et al., 1982a; Yu et al., 1991], while the sacculus of the squirrel monkey, under normal physiological conditions, has purely equilibrium function [Fernández and Goldberg, 1976a; Fernández et al., 1972], and the sacculus of the thornback ray has both acoustic and equilibrium function [Lowenstein and Roberts, 1950, 1951]. Thus, the homolog of an end organ that has acoustic sensitivity in one taxon may have equilibrium sensitivity in a second taxon and both acoustic and equilibrium sensitivity in a third taxon. From this, an intriguing question arises: what changes are involved in the evolutionary transition from one sensor type to the other? That is, what features make an acoustic sensor an acoustic sensor versus an equilibrium sensor and vice versa?

Traditionally, acoustic sensors and equilibrium sensors have been distinguished on the basis of the mode, frequency range, and amplitude of the stimuli to which they respond. Acoustic signals can be defined as mechanical waves that propagate in some medium and that carry information about their sources. Auditory signals, the most familiar type of acoustic signals, consist of sound waves through air or water. Seismic (or vibratory) signals, another class of acoustic signals, consist of waves that travel through solid media, usually the underlying substrate. Inner-ear acoustic sensors typically have been identified as those sensors that respond to mechanical stimuli of these types that are high in frequency (greater than approximately 10 Hz). Equilibrium signals can be defined as those that affect the orientation and motion of the animal's whole head. Ultimately, for the inner ear, these are stimuli that accelerate the head (either through translational or rotational motion), or that change the orientation of the head relative to the direction of the equivalent acceleration of gravity. Inner-ear equilibrium sensors typically have been identified as those that respond to stimuli of these types that are low in frequency (less than approximately 10 Hz) and large in amplitude – that is, disturbances low enough in frequency to allow for compensatory postural or oculomotor responses, and large enough in amplitude to affect an animal's orientation and motion.

It is possible that all that is necessary to switch an end organ from being an equilibrium sensor to being an acoustic sensor, or vice versa, is to endow it with access to the appropriate stimulus mode and frequency range, and to endow it with the appropriate sensitivity. Studies have shown that fibers from the saccular macula and semicircular canal cristae of mammals respond to intense (greater than approximately 100 dB SPL) auditory stimuli [Young et al., 1976, 1977; Didier and Cazals, 1989; McCue and Guinan, 1993, 1994]. If the hair cells of these equilibrium end organs had the appropriate access to acoustic excitation, it is possible that they could serve perfectly well as acoustic sensors. We wondered, however, if there were other features that distinguish these two sensor types – features that reflect fundamental differences in the underlying signal processing of the sensors themselves.

Evolutionary Considerations

It is reasonable to assume that inner-ear sensory systems persisted because of the selective advantages they conferred on individual organisms in extracting biologically relevant information from the available signals in the environment. Furthermore, it is reasonable to assume that their evolution was guided principally by selection mechanisms; that is, over the course of evolutionary time, selection forces have sculpted system features that increase system performance and in turn increase organismal fitness. One can then presuppose a system's adaptive function and from this, using certain guiding principles and considering physical constraints [Dullemeijer, 1970], deduce the system features (necessary to perform that function) that would tend to be selected for.

One might assume that the adapative advantage of an acoustic sensory system is its ability to infer information about the various objects emitting acoustic signals in an animal's environment. This is true especially for an auditory system. At any point in time, the total acoustic signal at an animal's ear is composed of the sum of many overlapping signals from the individual sources of acoustic waves in the environment – the advertisement call of a potential mate,

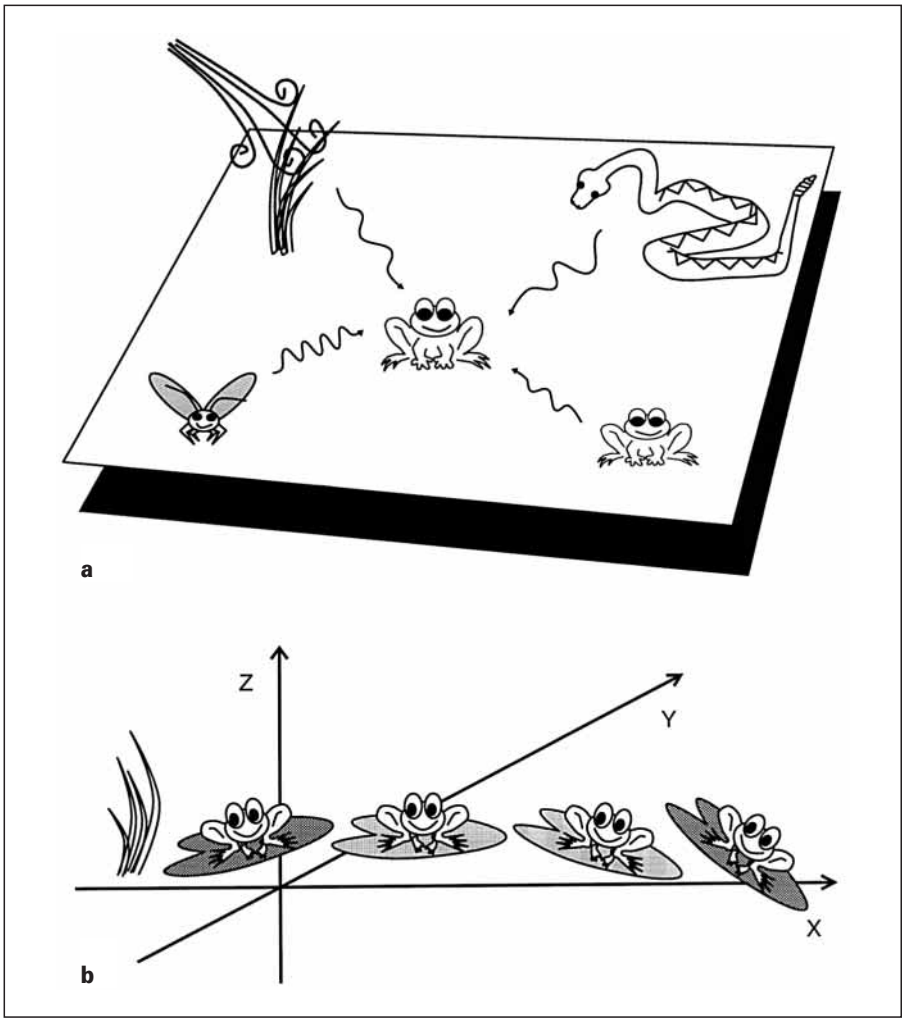

Fig. 1. This figure depicts the presumptive adaptive functions of the acoustic and equilibrium systems. **a** Acoustic stimuli comprise mechanical disturbances of the environmental media. The adaptive advantage of an acoustic system is in inferring information about the remote (acoustic) objects in an organism's environment – in this case, an approaching predator, a potential mate, a possible prey item, and the wind in the reeds. It is these individual acoustic sources that are of biological relevance to the animal; a well adapted acoustic system would be capable of sorting these individual signal components from the total acoustic signal. **b** Equilibrium stimuli comprise disturbances of animal head orientation and motion. The presumptive adaptive advantage of an equilibrium system is in inferring information about an organism's overall head motion and orientation. The overall equilibrium disturbance is represented schematically by head orientation in the coordinate space. It is this sum total orientation and motion that is of biological relevance to the animal; a well adapted equilibrium system need not be capable of accomplishing signal sorting according to individual sources.

the footfall of an approaching predator, the rustling of foliage in the wind (see fig. 1a). It is these individual signal components that convey the contents of the animal's immediate world. And it is these individual signal components, not the sum total acoustic signal, that are ultimately of biological relevance to the animal. One can argue then that an acoustic system must be capable of sorting this acoustic mêlée into separate signal components, each coming from an individual acoustic source.

Furthermore, one might assume that the adaptive advantage of an equilibrium system is its ability to infer an animal's own orientation and motion. Many separate sources of disturbance may contribute to the changes in the motion and orientation of the head (i.e., to the overall equilibrium signal at the ear), but one can argue that recognizing these individual sources is of little relevance to the process of generating compensatory eye or head movements. Is it really necessary that a floating amphibian discern the sources of disturbance that contribute to the rocking of her watery perch (see fig. 1b), or does she just need to compute her overall head motion and orientation in order to compensate correctly? Presumably it is only the overall equilibrium signal at the ear that is biologically relevant; the individual sources of disturbance that contribute to that signal are not. Thus, although it might be selectively advantageous for an equilibrium system to be able to decompose the overall equilibrium signal into components corresponding to a spatial basis set (e.g., roll, pitch and yaw), one can argue that the system need not be capable of sorting the overall equilibrium signal into components based on the individual sources of motion.

The following conclusion emerges: inner-ear acoustic sensors must have signal processing features consistent with accomplishing the task of sorting the total signal in-

put into components that correspond to individual signal sources, while inner-ear equilibrium sensors need not.

The Physical World and Constraints on Design

How can good signal sorting be achieved? When considering what sorts of signal-sorting schemes might have emerged in the evolving acoustic system, one might begin by considering what sorts of signal-sorting schemes signal-processing engineers have invented. The common feature of these schemes is decomposition of the total input waveform into a set of more basic parts.

Natural sounds can be divided on the basis of at least two dichotomies: (1) they are either transient or persistent, and (2) those that are persistent are either periodic or aperiodic. Periodic waveforms in nature, such as the vocalizations produced by many vertebrates, typically are produced by a relaxation process coupled to a resonance. If one decomposed such a periodic waveform in terms of spectral components (e.g., Fourier decomposition), there would be a very large number of such components, and they would be related harmonically – i.e., their frequencies would be integer multiples of the same fundamental frequency. Furthermore, all of these spectral components would begin together when the waveform commenced, and they would maintain constant phase relationships to one another – even in the presence of Doppler shifts. All spectral components would be subject to the same Doppler shifting (i.e., frequency modulation) owing to changes in the relative velocities of the source and listener. All spectral components would be subject to the same time-varying attenuating factors (e.g., changes in the orientation of the source, objects moving in and out of the sound path, etc.), and although the degree of amplitude modulation by such factors would depend on the frequency of the component, the basic temporal pattern of modulation would be the same for all components. Finally, sensed binaurally, all spectral components would exhibit the same interaural time difference.

Psychoacoustic studies have demonstrated that the properties described in the previous paragraph (harmonicity, common onset time, common amplitude-modulation pattern, common frequency-modulation pattern, and common interaural time difference) provide precisely the cues used by human listeners to segregate and integrate sounds of periodic waveforms into perceptual objects – that is, into sets of components inferred by neural computation to have arisen from individual acoustic sources [Hartmann, 1988; Yost, 1991]. Biological structures cannot perform true Fourier decomposition; they can, however, perform something similar to spectrographic decomposition. Each component of a spectrograph typically is derived by passing the signal to be analyzed through a distinct linear filter. This filter's properties can be described either in the frequency domain (in terms of its sinusoidal steady-state response) or in the time domain (in terms of its impulse response). An entire spectrograph would be produced by an array of such filters, each filter possessing a different frequency response and a correspondingly different impulse response. To allow for the detection of harmonicity, such an array would have to possess spectral resolution that was a small fraction of an octave. For example, detection of the sixth harmonic would require spectral resolution much better than 0.26 octave, the difference between the fifth and sixth harmonic. To allow for the detection of common onset times, on the other hand, the array would have to respond very quickly in time. Therefore, we expect the individual filters in the array performing spectrographic analysis to provide both good frequency discrimination and rapid temporal response to incoming signals.

There are two ways that signal-processing engineers can achieve good frequency discrimination in linear filters: (1) make the bandwidth of the filter extremely narrow, so that the filter responds preferentially to ongoing sine waves whose frequencies fall within a very narrow range; (2) make at least one band edge of the filter extremely steep, so that the responses of the filter to ongoing sine waves within its pass band are much greater than those to ongoing sine waves at frequencies beyond the steep band edge. The first method can be achieved with structures of low dynamic order – i.e., structures possessing a low number of interacting, independent energy storage elements (e.g., a low number of interacting masses and springs). Because low dynamic order implies a small number of structural elements, parsimony suggests that such a scheme would be favored in the evolution of inner-ear tuning structures. Unfortunately, in accomplishing tuning by reduction of bandwidth, one must sacrifice time resolution. In the context of the previous paragraph, this leads to two serious problems: (1) following the onset of a sine wave, the response of a narrow-band filter requires considerable time to develop, and that time increases as the bandwidth of the filter decreases, and (2) residual excitation in a narrow-band filter, such as that elicited by prior background noise or prior signals, requires considerable time to decay, and that time also increases as the bandwidth of the filter decreases. In other words, as one improves the frequency discriminability of a filter by narrowing its bandwidth, that filter becomes more sluggish in responding to new signals, and those signals must compete with increased interference by signals from the immediate past. These problems are not present in broad-band filters in which frequency discrimination is

achieved by steep band edges. In filters of this type, there is no trade-off between spectral acuity and time response. Therefore, for purposes of using both spectral and temporal cues to sort acoustic signals from one another (e.g., for tracking a given signal in an acoustic environment filled with noise and competing signals), an array of filters with broad pass bands and steep band edges would be the appropriate structure for performing spectrographic analysis.

Increased steepness of the band edge requires increased dynamic order in the filter structure; therefore, filters of this sort require high dynamic order. Furthermore, the properties of the many independent energy storage elements that create the filter's high dynamic order must be appropriately related to one another; and these elements must be appropriately connected to each other. In other words, for an engineer, the design of such a filter is not simple. Based on their presumptive adaptive advantages, however, one predicts that such high-order dynamics will be present in the acoustic sensors of the ear; and one expects the elements providing those dynamics to be organized appropriately to yield tuning curves with steep band edges.

Since equilibrium sensors need not be well suited to accomplishing signal sorting tasks, high-order dynamics become unnecessary. The features of an equilibrium sensor should, however, be consistent with detecting and transmitting information about total head motion and its simple derivatives (i.e., displacement, velocity, acceleration, and jerk). To detect motion of a rigid body, an engineer might employ an inertial element (sometimes called the sensing mass) coupled through an elastic element (spring) to the rigid body. The differential motion of the sensing mass and the rigid body that occurs when the latter is accelerated can be detected by strain gauges and ultimately translated into the various components of motion. The addition of a viscous element provides necessary damping of the mass-spring sensing system. Examples of such systems include conventional accelerometers and seismometers. Not surprisingly, the mechanics of inner-ear equilibrium sensors seem to be based ubiquitously on inertial sensing masses (solid in the otoconial end organs and fluid in the semicircular canals) attached to the head by a viscoelastic element [see Steinhausen, 1931, 1933; van Egmond et al., 1949; de Vries, 1950; and for reviews see Mayne, 1974; Wilson and Melvill Jones, 1979]. Based simply on these lumped mechanical elements, such a system inherently possesses second-order dynamics. Furthermore, since the ultimate stimulus to an inertial sensor is acceleration (either rotational acceleration, translational acceleration, or the equivalent translational acceleration of gravity), such sensors might be expected to have signal processing features that translate this acceleration into other simple components of head motion (i.e., displacement, velocity, or jerk). This task requires one or two steps of integration or differentiation with respect to time. Each energy storage element present in the system provides one such step. Thus the task would be accomplished well by systems with first-, second-, or third-order dynamics. Based on their presumptive adaptive advantage, one predicts that equilibrium sensors will possess linear tuning properties of such low dynamic order.

Previous Research on Tuning

Linear tuning properties have been observed for acoustic primary afferent nerve fibers from, for example, the cochlea in rats [Møller, 1977] and cats [de Boer and de Jongh, 1978; Carney and Yin, 1988; Evans, 1988], the sacculus and amphibian papilla in bullfrogs [Lewis, 1983, 1988; Yu et al., 1991], and the basilar papilla in turtles [Sneary and Lewis, 1989; Lewis et al., 1990]. The amplitude tuning curves obtained from these studies possess single pass bands with steep low- and high-frequency band edge slopes that imply dynamic orders ranging from five, in low-frequency axons of the basilar papilla in turtles, up to as high as 22, in mammalian cochlea. Do these steep slopes, and the high-dynamic order implied by them, reflect special adaptations in acoustic sensors as postulated, or are they simply inherent in all inner-ear sensors (including equilibrium sensors) excited in the frequency ranges of acoustic signals? With excitation at sufficiently high frequencies, the distributed properties of any real system emerge, and the dynamic order of the system will appear to be indefinitely high. To address the issue directly, we decided to examine the response dynamics of both acoustic and equilibrium primary afferent nerve fibers over the same frequency range; that is, over the frequency range of acoustic sensitivity.

Over the frequency ranges in which they have been most commonly observed (typically below 10 Hz) the linear tuning properties of vertebrate equilibrium sensors imply underlying structures of low dynamic order. Amplitude tuning curves have been published for primary afferent nerve fibers, for example, from the semicircular canal and otolithic end organs in squirrel monkeys [Fernández and Goldberg, 1971a, b, 1976b], frogs [Lowenstein and Saunders, 1975; Blanks and Precht, 1976; Caston et al., 1977; Myers and Lewis, 1991], cats [Anderson et al., 1978; Ezure et al., 1978], and chinchillas [Baird et al., 1988; Goldberg et al., 1990], and from the semicircular canals in rats and guinea pigs [Curthoys, 1982] and guitarfish [O'Leary and Honrubia, 1976]. Over these lower frequency ranges the observed linear tuning properties of the canal and otolithic equilibrium fibers implied underlying tuning structures of

low dynamic order (order one to three). Amplitude tuning curves over frequencies above 10 Hz have been obtained for afferent nerve fibers from semicircular canals in goldfish [Hartmann and Klinke, 1980] and pigeons [Dickman and Correia, 1989] using sinusoidal inputs. The amplitude tuning curves obtained in these studies also imply underlying tuning structures of low dynamic order. Other studies have been conducted which were aimed at determining whether or not equilibrium organs would respond to intense auditory stimuli. These studies examined the responses of the canal and sacculus in squirrel monkeys [Young et al., 1977], the canal in pigeons [Wit et al., 1984], and the sacculus in cats [McCue and Guinan, 1993], and they revealed V-shaped threshold tuning curves with intense best thresholds (greater than approximately 100 dB SPL) and slopes implying dynamic orders from three to six. To date, no amplitude tuning curves in the frequency range above 10 Hz have been published for a non-mammalian or non-avian vertebrate otoconial equilibrium sensor. Tuning curves from these end organs are of interest especially, because it is otoconial sensors that seem to have switched so many times over the course of evolution between equilibrium sensing and acoustic sensing. In fact, one otoconial organ in the bullfrog, the lagena, is notable for possessing both acoustic and equilibrium sensitivity, segregated into different regions of the sensory macula. We decided to exploit this organ to address our question regarding the dynamic order inherent in tuning structures at higher frequencies.

The Lagena

The function of the lagena has been studied in several vertebrate groups, and, like the sacculus, its functional character varies greatly across taxa. In thornback rays the lagena possesses equilibrium sensitivity [Lowenstein and Roberts, 1950, 1951]. In bony fish the lagena has primarily acoustic function [von Frisch, 1938; Furukawa and Ishii, 1967; and for review see Wever, 1974], though studies of lagenar fibers from flatfish have indicated that it may participate in both acoustic and equilibrium sensing [Platt, 1973, 1983; Platt and Popper, 1981]. In anuran amphibians, the lagena has both equilibrium and acoustic function. In other amphibians, as well as in reptiles, birds, and monotreme mammals, the function of the lagena is largely unknown. Central projections of primary afferent nerve fibers suggest that the lagena of reptiles has an auditory function [Hamilton, 1963] and that that of birds has both equilibrium and auditory functions [Boord and Karten, 1974; Boord and Rasmussen, 1963]. A physiological study, however, suggests that the lagena plays no role in auditory sensing in birds [Oeckinghaus, 1985].

The lagena of the North American bullfrog is a dorsoventrally oriented, otoconial end organ, unique among the inner-ear end organs of the bullfrog in sensing both acoustic (seismic) and equilibrium stimuli. The equilibrium response of the lagena in frogs (both *Rana temporaria* and *R. catesbeiana*) has been well characterized at frequencies up to 0.5 Hz, using stimuli consisting of stepwise or sinusoidal changes in head orientation (tilt) [Caston et al., 1977; Baird and Lewis, 1986]. Responses were measured in terms of changes in afferent spike rate. It was found that lagenar equilibrium fibers can be divided into three categories based on their response to changes in head orientation: (1) tonic fibers, which respond to static head orientation; (2) phasic fibers, which respond to the rate of change of head orientation, and (3) phasic-tonic fibers, which respond to both the rate of change of head orientation and static head orientation. The acoustic (seismic) response of the lagena in frogs has been demonstrated but it is not well characterized. It has been shown only that a population of fibers exists that do not respond to tilt stimuli but that do respond to light tapping of the substrate with bursts of spike activity [Narins, 1975; Caston et al., 1977]. The specific response characteristics of these fibers have not been determined. Feng et al. [1975] showed that the lagena is not responsive to airborne sound. Subsequent studies using the intracellular dye Lucifer Yellow CH [Stewart, 1978] have confirmed that the lagenar macula is the origin of both acoustic and equilibrium sensitive fibers [Baird et al., 1980; Lewis et al., 1982a; Baird and Lewis, 1986]. Furthermore, these studies and scanning electron microscope (SEM) studies [Lewis and Li, 1975] have revealed a relationship between afferent function, hair cell morphology, and location on the macula. The lagena is divided into functional and morphological bands along the length of the macula. The central band of the lagena striolar region (a strip about two hair cells wide) contains hair cells with bulbed kinocilia (Lewis and Li type E) and is the origin of seismic-sensitive nerve fibers. The parts of the striolar region outside this central band contain hair cells with short or long, unbulbed kinocilia (Lewis and Li type F and C) and are the origin of equilibrium phasic and phasic-tonic nerve fibers. The parts of the lagenar macula outside of the striolar region (the extrastriolar region) contain hair cells with very long, unbulbed kinocilia (Lewis and Li type B) and are the origin of equilibrium tonic fibers [Lewis and Li, 1975; Baird et al., 1980; Lewis et al., 1982a; Baird and Lewis, 1986]. Only primary afferent nerve fibers originating from the central band of the lagena striolar region show acoustic sensitivity. It is notable that the hair cells innervated by these seismic-sensitive nerve fibers are the only ones on the lagena to possess bulbed kinocilia. An

extremely small number of hair cells at the striolar region of the utricular macula are bulbed, but the functional character of fibers innervating these hair cells is not known [Baird and Lewis, 1986]. Otherwise, the only other sensory epithelia in the bullfrog's inner ear that possess hair cells with bulbed kinocilia are those with acoustic sensitivity; these end organs include the amphibian papilla, the basilar papilla (the two frog auditory end organs), and the sacculus [Lewis and Li, 1975].

To date, no amplitude tuning curves have been published for any primary afferent nerve fibers from the lagena in frogs. In this study, we used random vertical motion and correlation analysis to characterize the linear response dynamics of lagenar afferent nerve fibers over the frequency range from 10 Hz to 1.0 kHz. The tuning curves that we obtained typically extended to 500 Hz or more before they were obscured by noise. Amplitude tuning curves fell into two categories – those that possessed lowpass tuning properties, and those that possessed bandpass tuning properties. Dye-filling and tracing of single fibers from the lagenar branchlet indicated that lowpass units originated from equilibrium-sensitive regions of the macula, while bandpass units originated from seismic-sensitive regions of the macula. We calculated the low- and high-frequency slopes of these amplitude tuning curves in order to estimate and compare the dynamic orders of the underlying tuning structures for these two classes of fibers. In contrast with the dynamic orders implied by the amplitude tuning curves of lagenar bandpass (putative acoustic) fibers, which typically were four to six (and which went up to as high as nine), the dynamic orders implied by the amplitude tuning curves of lagenar lowpass (putative equilibrium) fibers typically were one or two (up to three). We conclude that high dynamic order is indeed a special feature of acoustic sensors, not shared by equilibrium sensors (at least in the bullfrog lagena), even when the latter are driven at acoustic frequencies.

Materials and Methods

The research reported here was carried out under the guidelines established by the Animal Care and Use Committee at the University of California, Berkeley. A more detailed description of the methods used in this study has been given elsewhere [see Cortopassi and Lewis, 1996]. The responses of primary afferent nerve fibers were recorded intra-axonally from either the lagenar branchlet or the posterior ramus of the VIIIth cranial nerve in North American bullfrogs *(Rana catesbeiana)*. Animals were mounted on a rigid platform, ventral side up, and stimulated with small-amplitude, dorsoventral translational motion [root-mean-square (RMS) displacements typically less than 0.5 μm]. The stimulus had Gaussian amplitude distribution. By means of graphic and parametric equalizers the stimulus was band-limited and adjusted to have a velocity spectrum that typically was flat to within ±3 dB for a frequency range of 10 Hz to 1.0 kHz. For these experiments, the RMS amplitude of the velocity stimulus was typically 2×10^{-5} m/s.

Discrete cross-correlation analysis and discrete Fourier transformation were used to estimate the linear tuning properties of the peripheral sensors associated with each afferent nerve fiber studied. Specifically, we used the reverse correlation (REVCOR) method which provides an estimate of the linear impulse response of the system being analyzed [see de Boer and Kuyper, 1968; de Boer and de Jongh, 1978; Eggermont, 1993; and for specific details of our system, Yu et al., 1991]. The corresponding amplitude and phase versus frequency tuning curves of the afferent nerve fibers were calculated by taking the discrete Fourier transform (DFT) of the estimated impulse response. For a sample of 26 fibers, the arbitrary impulse response amplitudes generated by our REVCOR system were converted to actual amplitudes in spikes per second per meter (spk/s/m). Input-output transfer ratios (akin to the gains of the amplitude tuning curves) were calculated for these same fibers. This was accomplished by equating the energy in a fiber's impulse response *h(t)* to the energy in its corresponding amplitude frequency response *H(f)* (i.e., equating the energy of a time domain signal to that of its Fourier transform):

$$\int_{-\infty}^{\infty} [h(t)]^2\, dt = \int_{-\infty}^{\infty} [H(f)]^2\, df.$$

For our analysis, this relationship becomes a summation:

$$\sum_{i=1}^{n} h_i^2 \Delta t = \sum_{i=1}^{n} H_i^2 \Delta f = \sum_{i=1}^{n} (T_R H_i')^2\, \Delta f = T_R^2 \sum_{i=1}^{n} (H_i')^2\, \Delta f$$

with $\Delta t = w/n$, $\Delta f = l/w$, where w is the REVCOR window length in seconds, n is the number of discrete-time bins (for these experiments $w = 100$ ms, $n = 1{,}024$), $H'(f)$ is the normalized amplitude frequency response obtained by REVCOR, and T_R is the input-output transfer ratio in spikes per meter (spk/m). Decibel (dB) values on a unit's normalized amplitude tuning curve are referenced to this transfer ratio.

The slopes of the amplitude tuning curves over selected low- and high-frequency ranges were estimated by least-mean-square fits to straight lines. A fiber's dynamic order was calculated from these slopes. When the low-frequency band-edge slope was negative or zero and the high-frequency band-edge slope was negative, the dynamic order was calculated as the absolute value of the high-frequency band-edge slope divided by 20 dB/decade and rounded to the nearest integer. When the low-frequency band-edge slope was positive and the high-frequency band-edge slope was negative, the dynamic order was calculated as the sum of the absolute values of the two band-edge slopes divided by 20 dB/decade and rounded to the nearest integer. The corner frequency of each lowpass fiber was taken to be the frequency at the intersection of the straight lines estimating the low- and high-frequency slopes. This corner frequency was also used to define the fiber's bandwidth. The pass band of each bandpass fiber was taken to be the frequency region demarcated by the low- and high-end frequencies $F_{low_{10\ dB}}$ and $F_{high_{10\ dB}}$ at which the tuning curve was approximately 10 dB below its maximum amplitude. We used 10 dB rather than 3 dB frequency values because fluctuations in the tuning curves due to noise were on the order of ±3 dB. The center frequency of each bandpass fiber was taken to be the frequency at the mid-point of the pass band of the amplitude tuning curve on the log scale and was calculated as $F_c = \sqrt{F_{low_{10\ dB}} \cdot F_{high_{10\ dB}}}$. The low- and high-end frequencies defining a fiber's pass band were used to calculate its bandwidth in octaves (or linearly in Hz).

After characterization of their linear tuning properties by REVCOR analysis, a small number of lagenar afferent nerve fibers were injected with the intracellular dye Lucifer Yellow CH. Filled fibers were examined under a fluorescence microscope and, if possible, a determination was made about their point of origin; that is, whether they originated from acoustic or equilibrium regions of the lagenar macula. This was done in order to relate amplitude tuning properties to a previously established map of sensory function over the various regions of the macula [Lewis et al., 1982a; Baird and Lewis, 1986].

Results

The fibers that we recorded from the lagenar macula could be divided into two categories – those possessing lowpass amplitude tuning characteristics and those possessing bandpass amplitude tuning characteristics. Lowpass amplitude tuning curves were roughly flat in response to velocity at lower frequencies, and they rolled off with gentle negative slope at higher frequencies. Bandpass amplitude tuning curves were roughly flat in response to velocity over a limited frequency range (the pass band), and they rolled off with steep slope at lower frequencies and higher frequencies (possessing constant positive slope at the low-frequency band edge and constant negative slope at the high-frequency band edge). In all, 44 such lowpass units were recorded, and 73 such bandpass units were recorded.

The lowpass fibers recorded were the focus of a previous paper [Cortopassi and Lewis, 1996]. The estimated low-frequency slopes of the amplitude tuning curves of these fibers ranged from –8 dB/decade to 9 dB/decade. The high-frequency slopes of the amplitude tuning curves ranged from –7 dB/decade to –63 dB/decade. The summed low- and high-frequency slopes (absolute values, summed only if the low-frequency slope was positive) ranged from 10 dB/decade to 64 dB/decade. The response dynamic orders calculated from these slopes were one (for 27 units), two (for 11 units), and three (for 5 units). The tuning curve of one unit implied dynamic order of 0.5 (suggesting some sort of distributed-parameter process [e.g., see Thorson and Biederman-Thorson, 1974]). Estimated corner frequencies for the amplitude tuning curves ranged from less than 10 Hz to 270 Hz. The corner frequency (f_c) of a fiber is related to its time constant (τ) by $\tau = 1/2\pi f_c$. The corner frequencies for 37 fibers ranged from 20 Hz to 150 Hz (corresponding to time constants ranging from 1.1 ms to 8.0 ms). The corner frequencies for three fibers ranged from 240 Hz to 270 Hz (corresponding to time constants ranging from 0.59 ms to 0.66 ms). The corner frequencies for the four remaining fibers were below 10 Hz (corresponding to time constants greater than 16 ms). Input-output transfer ratios were calcu-

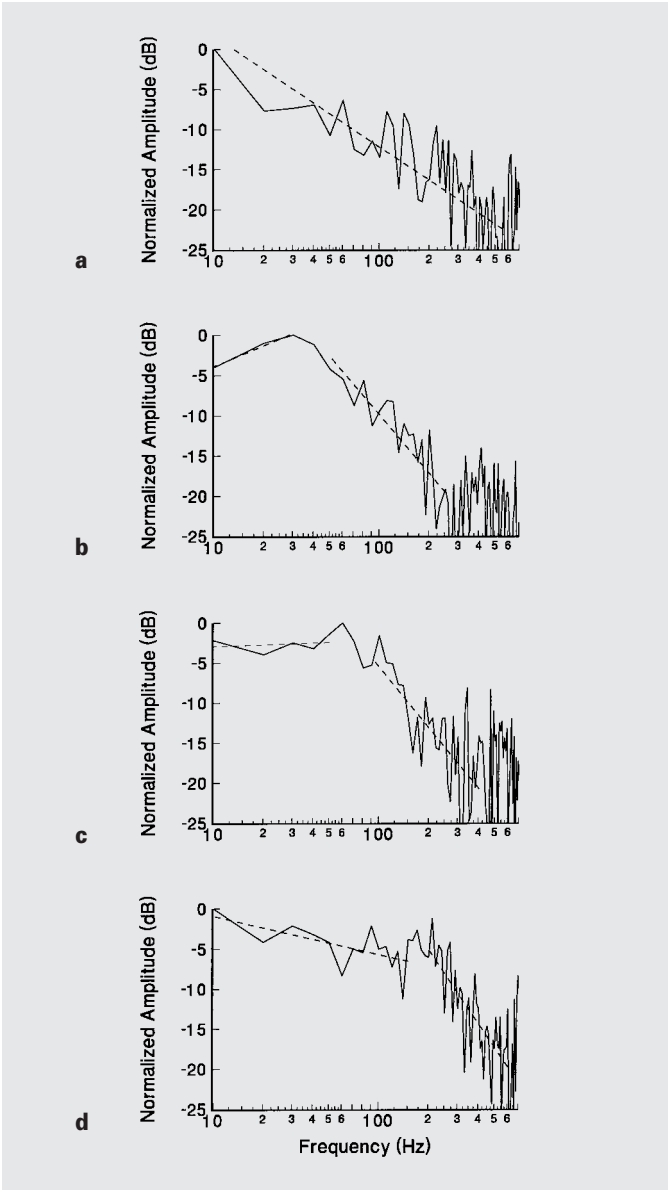

Fig. 2. Amplitude tuning curves of four lowpass units, each possessing a different corner frequency: <10 Hz (**a**), 40 Hz (**b**), 75 Hz (**c**), and 240 Hz (**d**). Unit dynamic orders equal: one (–14 dB/decade slope over the entire stimulus frequency range) (**a**), two (9 dB/decade low-frequency slope, –24 dB/decade high-frequency slope) (**b**), one (1 dB/decade low-frequency slope, –25 dB/decade high-frequency slope) (**c**), and two (–5 dB/decade low-frequency slope, –31 dB/decade high-frequency slope) (**d**). The unit corner frequencies correspond to time constant of >16 ms (**a**), 4.0 ms (**b**), 2.1 ms (**c**), and 0.66 ms (**d**).

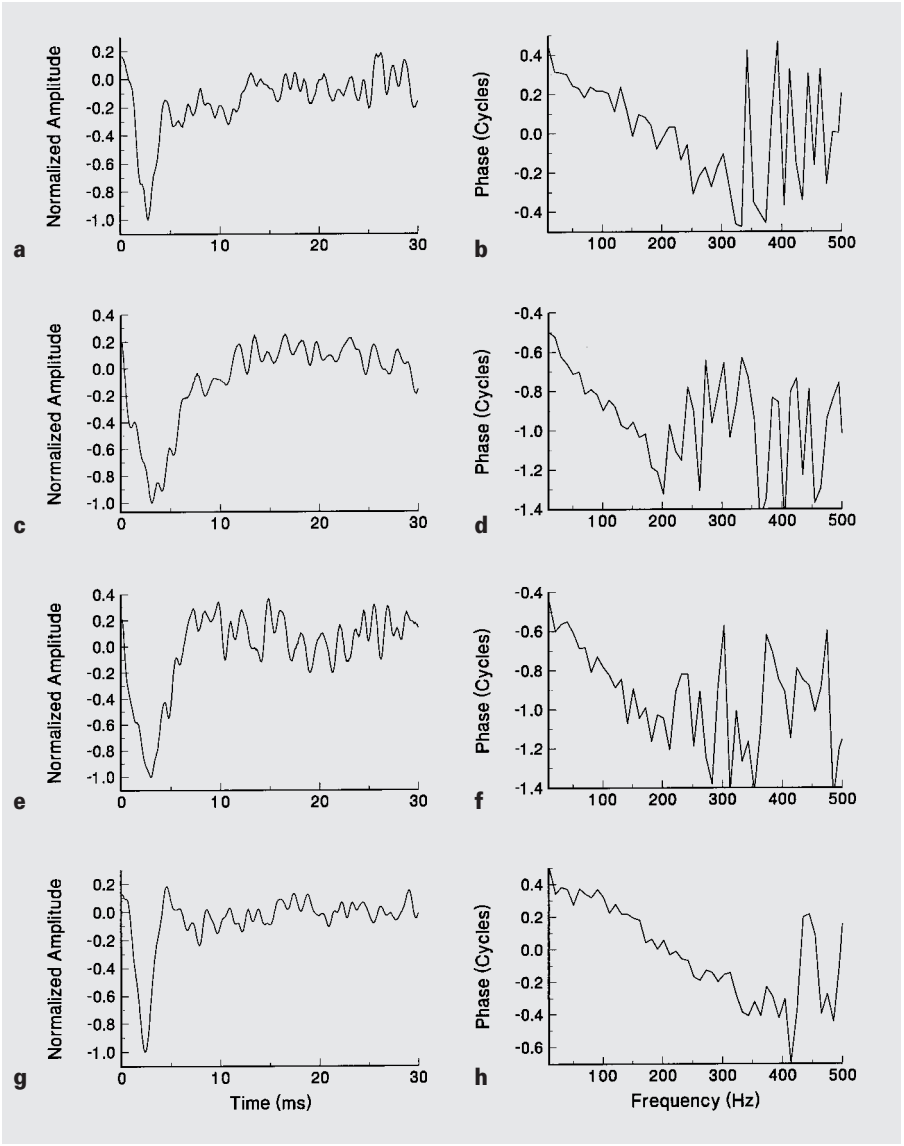

Fig. 3. The impulse response curves (**a**, **c**, **e**, **g**) and phase versus frequency tuning curves (**b**, **d**, **f**, **h**) for the four lowpass fibers of figure 2.

lated for a sample of 13 lowpass units. The transfer ratios of the amplitude tuning curves ranged from 0.30 spk/µm to 1.74 spk/µm for 12 of these 13 fibers. The other fiber possessed a maximum gain of 4.18 spk/µm. The product of input-output transfer ratio and (linear) bandwidth (akin to the gain-bandwidth product of the amplitude tuning curve) was also calculated for these 13 units. Gain-bandwidth products ranged from 8.40 Hz·spk/µm to 466 Hz·spk/µm with 11 of the 13 fibers possessing gain-bandwidth products less than 200 Hz·spk/µm. Figure 2 shows the amplitude tuning curves of four different lowpass units, each possessing a different corner frequency (giving a sample of the range of corner frequencies that we encountered). The impulse responses and phase tuning curves of these units are shown in figure 3.

For the 73 bandpass fibers recorded, the estimated low-frequency slopes of the amplitude tuning curves ranged from 16 dB/decade to 101 dB/decade. The high-frequency slopes of these amplitude tuning curves ranged from –29 dB/decade to –123 dB/decade. The summed low- and high-frequency slopes (absolute values) ranged from 53 dB/decade to 185 dB/decade. The response dynamic orders estimated from these combined slopes were three (for 8 units), four (for 18 units), five (for 29 units), six (for

15 units), eight (for 2 units), and nine (for 1 unit). The pass bands of these amplitude tuning curves were rather broad. Fiber bandwidths ranged from 1.2 octaves to 4.0 octaves, with the typical bandwidth being roughly three octaves. These pass bands centered on frequencies ranging from 46 Hz to 215 Hz. For 28 units, the center frequencies were less than 100 Hz, for 42 units, the center frequencies were between 100 Hz and 200 Hz, and for the remaining 3 units, the center frequencies were greater than 200 Hz. Input-output transfer ratios calculated for a sample of 13 bandpass units ranged from 0.40 spk/µm to 6.46 spk/µm with 8 of the 13 fibers having transfer ratios greater than 2 spk/µm. The gain-bandwidth products of these amplitude tuning curves ranged from 124 Hz·spk/µm to 1,912 Hz·spk/µm with 12 of the 13 fibers possessing gain-bandwidth products greater than 200 Hz·spk/µm. Figure 4 shows the amplitude tuning curves for three different bandpass units, each centered on a different frequency (giving a sample of the range of band centers that we encountered). The impulse responses and phase tuning curves of these units are shown in figure 5.

After characterization of their linear tuning properties by REVCOR analysis, a small number of lagenar afferent nerve fibers were injected with the intracellular dye Lucifer Yellow CH. Four of the recorded fibers were traced back to their origins on the lagenar macula [these results have been discussed previously; see Cortopassi and Lewis, 1996]. Three of these fibers were found to originate from areas of the striolar region well outside of the acoustic central band, areas previously identified as the origins of phasic and phasic-tonic lagenar equilibrium fibers [Lewis et al., 1982a; Baird and Lewis, 1986]. All three fibers possessed lowpass, low-order response dynamics; the estimated dynamic orders were three, one, and one. The other fiber was found to originate from the central band of the striolar region. This region was previously identified as the origin of lagenar acoustic (seismic) fibers [Lewis et al., 1982a; Baird and Lewis, 1986]. This unit showed bandpass, high-order response dynamics; its estimated dynamic order was six. These results corroborate our presumption that lowpass, low-dynamic-order units correspond to lagenar equilibrium fibers, and bandpass, high-dynamic-order units correspond to lagenar acoustic (seismic) fibers.

Figure 6 shows the results of REVCOR analysis for a lowpass (putative equilibrium) fiber and a bandpass (putative acoustic) fiber recorded from the lagenar branchlet [redrawn from Cortopassi and Lewis, 1996]. While the REVCOR-derived tuning curves of lowpass fibers tended to be more noisy, in general, than those of bandpass fibers, the amplitude tuning curve of this lowpass fiber was especially clean. Its summed low- and high-frequency slope

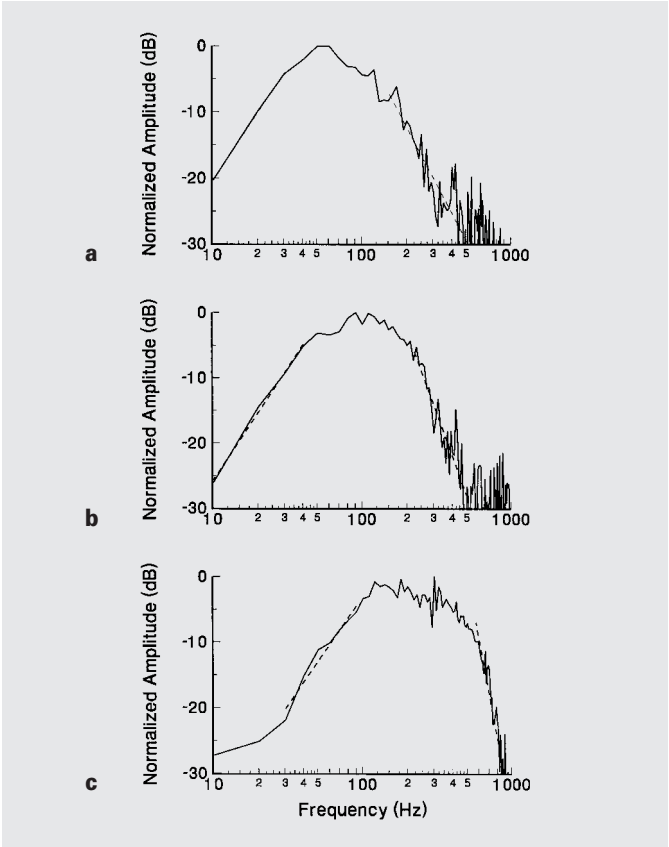

Fig. 4. Amplitude tuning curves of three bandpass units, each possessing a different band-center frequency: 60 Hz (**a**), 100 Hz (**b**), and 200 Hz (**c**). Unit dynamic orders equal: four (34 dB/decade low-frequency slope, –43 dB/decade high-frequency slope) (**a**), five (35 dB/decade low-frequency slope, –64 dB/decade high-frequency slope) (**b**), and eight (33 dB/decade low-frequency slope, –123 dB/decade high-frequency slope) (**c**).

(38 dB/decade) yielded an estimated dynamic order of two. The summed low- and high-frequency slope (165 dB/decade) of the bandpass fiber yielded an estimated dynamic order of eight. The estimates of dynamic order made from the amplitude tuning curves were corroborated by the phase tuning curves. A fiber's dynamic order also can be estimated from its phase tuning curve by dividing the total range of phase shift over the frequency range by 0.25 cycle. The lowpass unit showed a total phase lag of 0.45 cycle (giving an estimate for dynamic order of 1.8). The bandpass unit showed a total phase lag of 1.95 cycles over the frequency range (giving an estimate for dynamic order of 7.8). In general, however, the order estimated from a fiber's phase tuning curve did not match the order estimated from its amplitude tuning curve; the order estimated from phase tuning

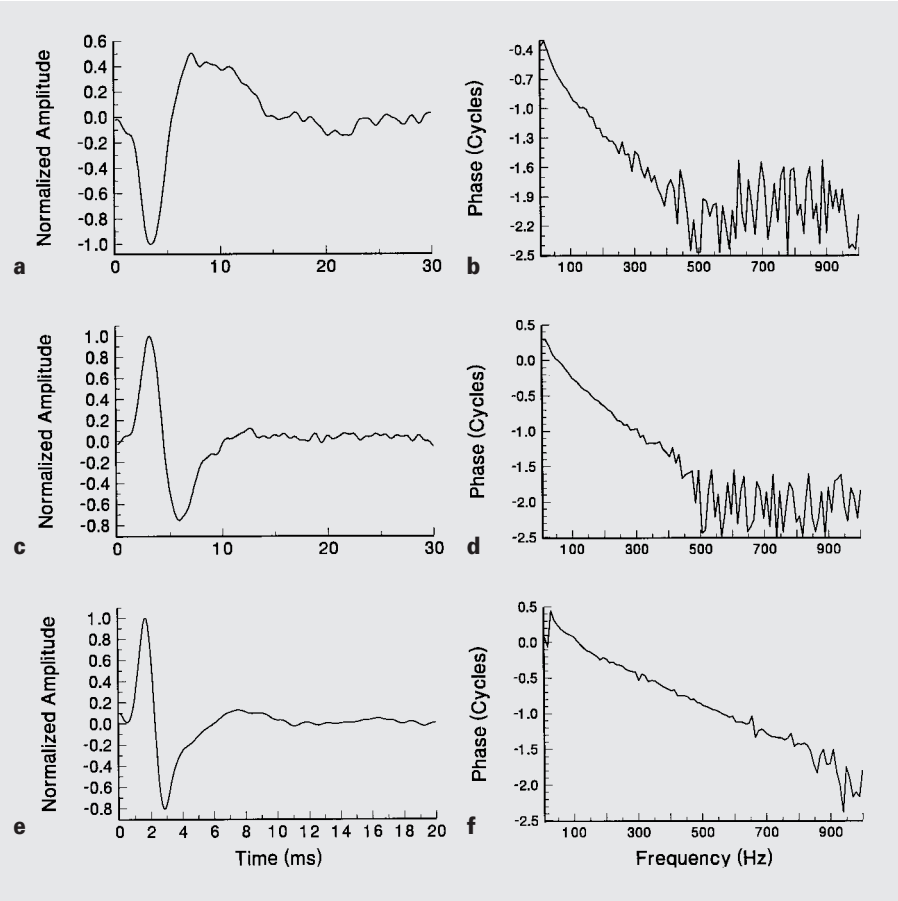

Fig. 5. The impulse response curves (**a**, **c**, **e**) phase versus frequency tuning curves (**b**, **d**, **f**) for the three bandpass fibers of figure 4.

curves tended to be higher. This higher total range of phase shift and thus higher estimate of dynamic order (than that expected from the amplitude tuning curve) could be due to a time delay element (Δt) in series with the peripheral tuning structure. A time delay element passes all frequencies equally (and thus does not affect the overall amplitude tuning curve); it does, however, add a phase lag of $-\Delta t\ \omega$ to the phase tuning curve. For a total frequency range of examination equal to $\Delta\ \omega$, a time delay of Δt adds a phase shift of $-\Delta t\ \Delta\ \omega$ to the total range of phase shift on the phase tuning curve; thus the estimate of dynamic order increases by $\Delta t\ \Delta\omega/0.25$ over that frequency range. Finally, one should note the conspicuous difference in the shape of the impulse response curve obtained for the lowpass unit with that of the impulse response curve obtained for the bandpass unit. This difference between impulse response curves is also seen when comparing the impulse responses of the lowpass units in figure 3 with the impulse responses of the bandpass units in figure 5. Impulse response curves for lowpass fibers consistently were monophasic (that is, they were mostly below, or in some cases above, zero), while those for bandpass fibers consistently were biphasic (that is, they were symmetric about zero). This observed difference is to be expected and can be seen from the convolution integral $y(t) = \int_0^t h(\tau)x(t-\tau)\delta\tau$ which relates the output $y\ (t)$ to the input $x\ (t)$ and the system impulse response $h\ (t)$. For a system that attenuates low frequencies (such as a bandpass filter), the output in response to a DC input [i.e., $x\ (t)$ equal to a constant] should be zero (or close to zero). For a DC input, the convolution integral will go to zero only if the area under the impulse response curve $h\ (t)$ integrates to zero (i.e., only if the curve has roughly equal area above and below zero).

Figure 7 shows the distribution of estimated dynamic orders for all 117 lagenar afferent nerve fibers recorded. It is clear that lowpass (equilibrium) units from the bullfrog lagenar macula have conspicuously lower dynamic orders than bandpass (acoustic) units. The modal value of dynamic order estimated for lowpass units was one, while the modal value of dynamic order estimated for bandpass units was five. Table 1 summarizes all tuning properties estimated for the lowpass and bandpass fibers.

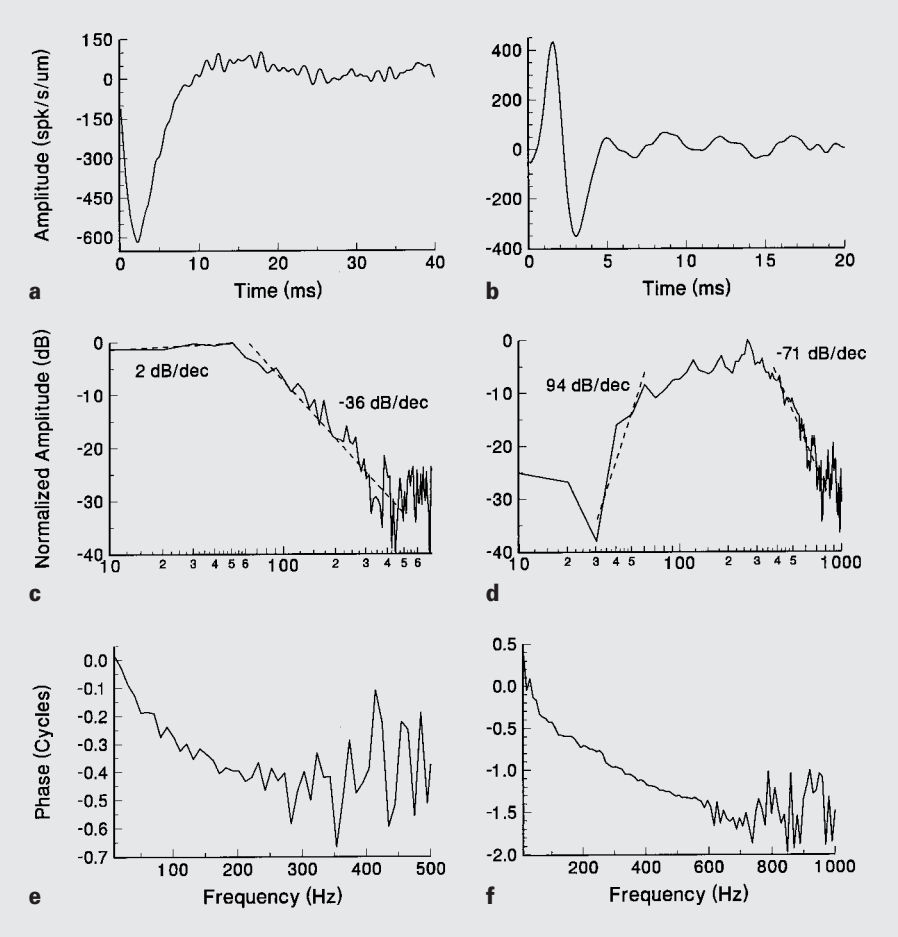

Fig. 6. The impulse response curves (**a**, **b**), amplitude tuning curves (**c**, **d**), and phase tuning curves (**e**, **f**) for a lowpass (putative equilibrium) and bandpass (putative acoustic) unit recorded from the lagenar branchlet. Combined slopes of the lowpass amplitude tuning curve (**c**) imply an underlying tuning structure of dynamic order two (2 dB/decade low-frequency slope, –36 dB/ decade high-frequency slope); with a 60 Hz corner frequency, 4.18 spk/µm transfer ratio, and corresponding 259 Hz·spk/µm gain-bandwidth product. Combined slopes of the bandpass amplitude tuning curve (**d**) imply an underlying tuning structure of dynamic order eight (94 dB/decade low-frequency slope, –71 dB/decade high-frequency slope); with a 163 Hz band center frequency, 3.0 octave (411 Hz) bandwidth, 1.48 spk/µm transfer ratio, and corresponding 608 Hz·spk/µm gain-bandwidth product.

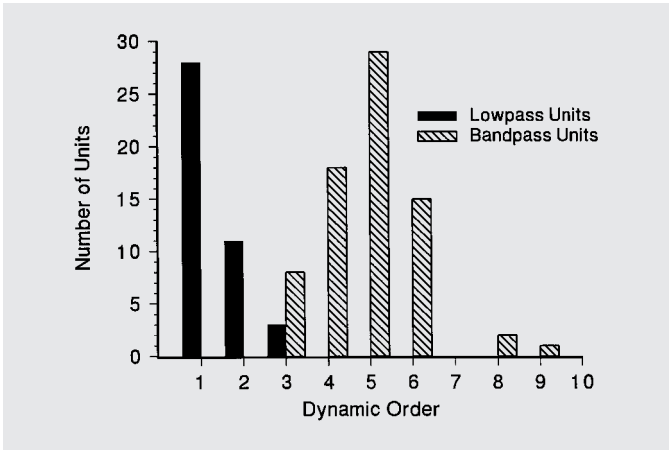

Fig. 7. Distribution of estimated dynamic orders for 117 afferent nerve fibers from the bullfrog lagena. Notice that lagenar lowpass (putative equilibrium) fibers possessed distinctly lower dynamic orders than lagenar bandpass (putative acoustic) fibers. The modal dynamic order for lowpass units was one. The modal dynamic order for bandpass units was five.

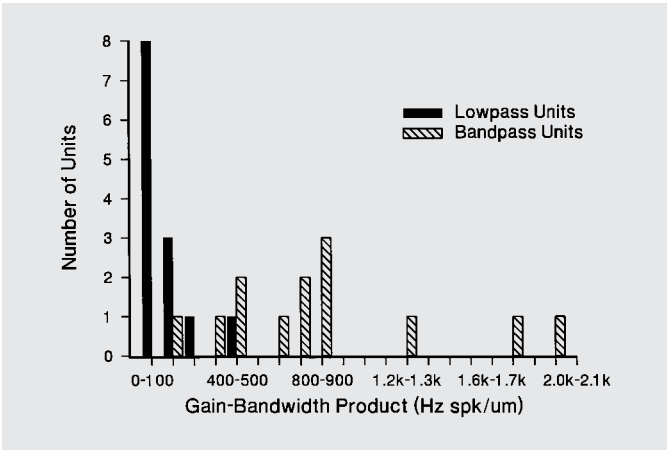

Fig. 8. Distribution of gain-bandwidth products for a sample of 26 afferent nerve fibers from the bullfrog lagena. Notice that lowpass (putative equilibrium) fibers possessed distinctly lower-gain-bandwidth products than bandpass (putative acoustic) fibers. Eleven of 13 lowpass fibers possessed a gain-bandwidth product less than 200 Hz · spk/µm, while 12 of 13 bandpass fibers possessed a gain-bandwidth product greater than 200 Hz · spk/µm.

Table 1. Comparison of the ranges of linear tuning properties for the populations of lagenar lowpass (putative equilibrium) and bandpass (putative acoustic) fibers recorded

	Lowpass tuning curves (44 fibers)	Bandpass tuning curves (73 fibers)
Low-frequency slope	–8 to 9 dB/dec	16 to 101 dB/dec
High-frequency slope	–7 to –63 dB/dec	–29 to –123 dB/dec
Summed slope	10 to 64 dB/dec	53 to 185 dB/dec
Dynamic order	one to three	three to nine
Modal value	one	five
Input-output transfer ratio	0.30 to 4.18 spk/µm	0.40 to 6.46 spk/µm
Gain-bandwidth product	8.40 to 466 Hz · spk/µm	124 to 1,912 Hz · spk/µm
Corner frequency	<10 to 270 Hz	–
Band center frequency	–	46 to 215 Hz
Bandwidth	–	1.2 to 4.0 oct
	<10 to 270 Hz	106 to 541 Hz

While there is not a highly pronounced distinction, lowpass units tended to possess lower input-output transfer ratios than bandpass units. The typical transfer ratio for lowpass units was between 0 and 1 spk/µm, while the typical transfer ratio for bandpass units was between 2 and 3 spk/µm. Furthermore, the majority of lowpass units (12/13) possessed transfer ratios below 2 spk/µm, while the majority of bandpass units (8/13) possessed transfer ratios above 2 spk/µm. The gain-bandwidth product, however, was distinctly higher for bandpass units than for lowpass units. The majority of lagenar lowpass fibers (11/13) possessed a gain-bandwidth product less than 200 Hz·spk/µm. The majority of lagenar bandpass fibers (12/13) possessed a gain-bandwidth product greater than 200 Hz·spk/µm. The typical gain-bandwidth product for lowpass units was between 0 and 100 Hz·spk/µm, while the typical gain-bandwidth product for bandpass units was between 800 and 900 Hz·spk/µm. Thus, while lagenar acoustic fibers generally possess higher input-output transfer ratios than lagenar equilibrium fibers, we see that input-output transfer ratio was not increased at the expense of sensor bandwidth. Figure 8 shows the distribution of calculated gain-bandwidth products for these 26 lagenar fibers.

Discussion

We examined the responses of 117 primary afferent nerve fibers from the bullfrog lagenar macula over a frequency range spanning that to which other frog acoustic fibers (i.e., those from the sacculus and the amphibian papilla [Lewis et al., 1982b; Lewis, 1983, 1988; Yu et al., 1991]) are known to respond. We found that these lagenar afferent nerve fibers could be divided into two groups: (1) those with lowpass, low-dynamic-order tuning, and (2) those with bandpass, high-dynamic-order tuning. Our results imply that equilibrium sensors and acoustic sensors can be distinguished on the basis of the dynamic order of their underlying tuning structures, with putative equilibrium sensors possessing low-order dynamics, and putative acoustic sensors possessing high-order dynamics. Furthermore, these results strongly imply that (at least in the bullfrog lagena) the steep band-edge slopes of acoustic fibers, made possible by the high-order dynamics, are special adaptations of acoustic sensors for acoustic sensing, not simply inherent in all otoconial sensors excited in the higher acoustic frequency range. These results are consistent with the hypothesis that high-dynamic-order tuning is an evolutionary adaptation of acoustic sensors, possibly arising from the selective pressure to accomplish signal sorting tasks based on individual acoustic sources. Since each unit of dynamic order in a system requires the presence of one independent energy storage element (e.g., a system of dynamic order five will possess five such independent energy storage elements), the underlying tuning structure of a sensor possessing high dynamic order will be composed of many more connected independent energy storage elements than that of a sensor possessing low dynamic order. Thus, high-dynamic-order systems possess greater complexity than low-dynamic-order systems. The results of this study suggest that the evolutionary transition between equilibrium sensing and acoustic sensing involved not simply gaining access to the appropriate stimuli and frequency ranges but a significant shift in system dynamic order and thus system complexity.

Another feature that appears to distinguish lagenar acoustic fibers from lagenar equilibrium fibers is their input-output transfer ratios. From the sample of 26 fibers for

which transfer ratios were calculated, it appears that bandpass (putative acoustic) fibers possess amplitude tuning curves with slightly higher transfer ratios than lowpass (putative equilibrium) fibers. Furthermore, for a given stimulus amplitude level and number of data samples used to generate the REVCOR function, the amplitude tuning curves obtained for bandpass fibers were, in general, much cleaner than those obtained for lowpass fibers. In other words, the neural response of acoustic fibers was much more strongly correlated (i.e., phase-locked) to the dorsoventral translational motion stimulus than that of equilibrium fibers. For example, the amplitude tuning curves in figures 2c and 4b were both obtained at a stimulus amplitude level of 2×10^{-5} m/s, using roughly 2,500 spikes to generate the REVCOR function. Notice how the impulse response curve and corresponding amplitude tuning curve of the bandpass fiber (fig. 5c and 4b, respectively) are much cleaner (i.e., have a much lower noise floor) than those of the lowpass fiber (fig. 3e and 2c). The amplitude tuning curves obtained for lagenar lowpass fibers showed only roughly 20 dB of clean response before dropping into the noise (a 20 dB dynamic range), while those obtained for bandpass fibers showed 30 dB or more of clean response.

The high dynamic order seen in lagenar acoustic fibers is ubiquitous among fibers of the other acoustic sensors of the bullfrog inner ear. REVCOR-derived tuning curves from the bullfrog sacculus and amphibian papilla all exhibit bandpass tuning properties, and their observed dynamic orders typically are even higher (eight or greater) than those of bandpass lagenar units. These two end organs respond to both airborne sound and to substrate-borne vibration [Yu et al., 1991], and they seem to partition the acoustic frequency range – saccular units are tuned largely to frequencies below 100 Hz and amphibian papillar units are tuned to frequencies above 100 Hz. Bandpass units from the lagena are sensitive to substrate-borne vibration but not to airborne sound at behaviorally or physically relevant levels [Feng et al., 1975]. They have tuning pass bands that are conspicuously broader than those of saccular and amphibian papillar units, and they are tuned to frequencies that cover the ranges of both the sacculus and the amphibian papilla. The REVCOR-derived impulse responses of lagenar bandpass units are biphasic, as are those of approximately 60% of saccular units. The remaining saccular units exhibit impulse responses with multiple cycles (ringing), as do all amphibian papillar units. Their very broad pass bands give lagenar bandpass units much greater temporal resolution than that exhibited by saccular or amphibian papillar units. This is reflected in their impulse response curves, which are of conspicuously shorter duration than those of saccular and amphibian papillar units.

The Role of Bandpass Tuning in Seismic Sensors

Interestingly, while the dynamic orders of lagenar acoustic fibers were routinely higher than those of lagenar equilibrium fibers, the dynamic orders of these seismic fibers were not as high as the dynamic orders that have been observed previously in the auditory fibers of many vertebrates. Dynamic orders greater than twenty are common, for instance, in mammalian auditory fibers [Møller, 1977; de Boer and de Jongh, 1978; Carney and Yin, 1988; Evans, 1988]. These tuning properties are highly consistent with what would be expected of a tuning structure sculpted by evolutionary forces to achieve both high frequency-acuity and high temporal-acuity, the two requisites of good signal sorting. While the tuning properties of lagenar seismic fibers are consistent with preserving both time and frequency information, they appear to be (because of their shallower band-edge slopes) not as keenly suited as mammalian auditory fibers to the task of signal sorting. One can hypothesize that the pressure to accomplish signal sorting based on individual acoustic sources was not as strong a selective pressure on lagenar seismic sensors as it was on many auditory sensors. While the evolutionary arguments outlined in the introduction provide a good heuristic approach to exploring the differences in signal processing features between acoustic sensors and equilibrium sensors, and while they may indeed be important in accounting for the observed differences between auditory sensors and equilibrium sensors, it seems likely that there were other adaptive pressures (more relevant than the pressure to accomplish signal sorting) working to sculpt the higher-order, bandpass tuning properties of vertebrate seismic sensors.

To further contemplate the evolutionary forces that sculpted vertebrate inner ear seismic sensors, we ask the following question: what are the challenges that confront a sensory system detecting signals borne in the substrate; that is, what are the contours of the seismic landscape that a sensory system must navigate? Geologic surveys have revealed that for frequencies lower than approximately 10 Hz, the microseismic noise at the earth's surface increases sharply, following a $1/f^2$ function [Brune and Oliver, 1959; Frantti et al., 1962]. The ability to filter out this noise, noise that could interfere with the detection of biologically relevant signals, would indeed be an advantageous feature for a seismic sensor to possess. In all cases, the low-frequency band edges of the lagenar bandpass units that we recorded began rolling off at frequencies well above 20 Hz. This low-frequency roll-off helps to reduce the low-frequency ($1/f^2$) seismic noise inherent in the substrate. Further, what is the expected spectrum of a biologically relevant seismic signal? Lewis and Narins [1985] examined the frequency

spectrum of seismic signals (thumps) emitted by the white-lipped frog of Puerto Rico *(Leptodactylus albilabris)* during its call. The signal energy in these thumps lies predominantly between 20 Hz and 70 Hz. This spectrum is typical of that made by an impulsive seismic stimulus in moist soil (that is, made by something striking the soil surface such as a footdrum or a footfall). Figure 9a shows the spectrum of an artificial thump (generated with a lab-built striking device) recorded in the moist soil of Puerto Rico. The high-frequency band edges of all the lagenar seismic fibers we recorded began rolling off starting at frequencies of about 100 Hz (up to roughly 500 Hz). This high-frequency roll-off (like the low-frequency roll-off) helps to reduce seismic noise at frequencies outside of the relevant biological range, in this case, outside of the spectral range of an impulsive seismic stimulus. The pass bands of lagenar seismic fibers closely match the frequency spectrum of typical seismic signals; signal energy in the relevant frequency range is passed relatively unattenuated, and signal energy outside of the relevant frequency range is severely reduced by the steep band-edge slopes (see fig. 9b). These results are consistent with the hypothesis that high-order, bandpass tuning properties are a special feature of seismic sensors to help eliminate substrate noise which could interfere with the detection of the biologically relevant signals and that the pressure to increase signal to noise ratio was important in the evolution of vertebrate seismic sensors.

The pressure to accomplish signal sorting, however, also may have been a factor in the evolution of vertebrate seismic sensors. For instance, we found that lagenar seismic fibers were not all tuned to the same frequency band. Rather, the pass bands of the 73 bandpass amplitude tuning curves that we recorded covered different frequency regions over the 10 Hz to 1.0 kHz range, with band center frequencies ranging from 46 Hz to 215 Hz – a span of 2.2 octaves. This implies that some degree of spectrographic analysis and thus spectral sorting could be accomplished by a seismic sensory system possessing these peripheral tuning structures. Furthermore, previous studies have revealed that various vertebrate species can detect and localize seismic signals. For example, it was found that the sandswimming lizard *(Scincus scincus)* detects and localizes the seismic signals produced by insect prey items moving on the sand surface [Hetherington, 1989]. As well, the fire-bellied toads (*Bombina bombina* and *B. orientalis*) can orient to the source location of water surface waves [Walkowiak and Münz, 1985]. These anurans produce water surface waves (a type of seismic surface wave) and presumably use them in the establishment and maintenance of territories.

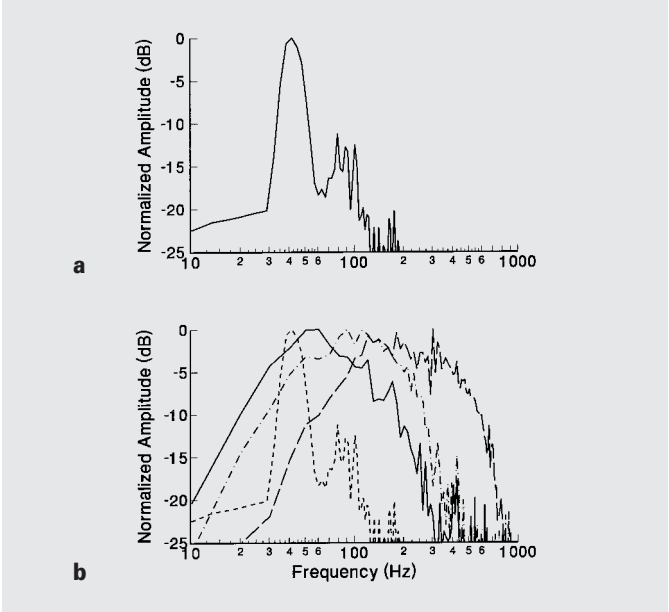

Fig. 9. The amplitude spectrum of an impulsive seismic stimulus in moist soil (measured with a vertically-oriented geophone) (**a**). This seismic spectrum is plotted with the amplitude spectrums (amplitude tuning curves) of three different bandpass fibers (the same fibers shown in fig. 4) from the bullfrog lagena (**b**).

Finally, based on their dynamic orders, the frequency resolution of lagenar seismic fibers should be comparable or roughly comparable to that of auditory fibers from other non-mammalian vertebrate inner ears. Auditory fibers from the basilar papilla of the red-eared turtle, for instance, exhibit dynamic orders ranging from four to seven [Sneary and Lewis, 1989; Lewis et al., 1990], and seismic-auditory fibers from the bullfrog sacculus and amphibian papilla exhibit dynamic orders ranging from eight to eleven; these are comparable to the dynamic orders ranging from three to nine that we measured for lagenar seismic fibers. While saccular and amphibian papillar units possess slightly steeper band-edge slopes (i.e., slightly higher dynamic orders), giving them improved frequency acuity, lagenar units possess slightly broader pass bands, giving them improved temporal acuity. It may be the case that for sensing environmental seismic stimuli, the lagena and the sacculus and amphibian papilla of the bullfrog partition time and frequency processing. That is, lagenar seismic sensors may have been selected specifically for increased resolution of the temporal structure of an incoming signal, while saccular and papillar sensors may have been selected for increased resolution of the spectral structure of the signal. While there may be some trade-offs between time and frequency pro-

cessing in these three sensors, all of them still possess good resolution in both domains.

Further Considerations of Equilibrium End Organs

A substantial number of the equilibrium units that we recorded had dynamic orders of one only. The minimum dynamic order expected of a system based on the mechanics of an inertial motion sensor (with the tuning curve measured relative to acceleration) is dynamic order two. To translate the velocity amplitude tuning curves that we obtained for lagenar equilibrium fibers into acceleration amplitude tuning curves, one must add –20 dB/decade to all slopes. For lowpass amplitude tuning curves (but not for bandpass tuning curves), this means that the low-frequency region that was roughly flat now has a slope of –20 dB/decade, and the high-frequency region that had a constant negative slope now has a slope –20 dB/decade steeper (that is, more negative by 20). This increases the dynamic order estimated over the frequency range by one; those fibers possessing dynamic order one with respect to velocity actually possess dynamic order two with respect to acceleration, as expected for the simplest inertial motion sensors. One should note also that the estimates of dynamic order made in this project are limited to the given frequency range of observation (i.e., 10 Hz to 1.0 kHz). An estimated dynamic order of *n* for a fiber implies that there are *n* time constants of the underlying tuning structure that can effect tuning in that frequency range. We were not able to observe additional slopes of the amplitude tuning curves at frequencies lower than 10 Hz and higher than 1.0 kHz (corresponding to time constants greater than 16 ms and less than 0.16 ms, respectively). Because, driven to indefinitely high frequencies, all real macroscopic structures will exhibit indefinitely high dynamic order, it is not the presence of dynamic order itself that is impressive, but the fact that *n* independent energy storage elements have been organized, not randomly but specifically in a way that creates a very effective filter for spectrographic analysis with good temporal resolution.

Conclusion

In this paper, we examined the question of what feature changes, specifically what changes in the tuning properties of peripheral sensors, accompany the evolutionary transition from equilibrium sensing to acoustic sensing (and vice versa) in the inner ear of vertebrates. The specific question we addressed (as a way to approach the more general question) was this: are the steeply-sloped bandpass amplitude tuning curves, corresponding to underlying tuning structures of high dynamic order, observed for acoustic sensors simply inherent in all vertebrate otoconial sensors excited in the frequency range from 10 Hz to 1.0 kHz? The data gathered here clearly imply that the answer is no. Lagenar acoustic sensors are tuned by means of peripheral structures with markedly greater dynamic order and thus greater physical complexity than lagenar equilibrium sensors. We conclude that high-dynamic order, bandpass tuning properties are indeed a special adaptation of acoustic sensors (possibly arising from the selective pressure to accomplish signal sorting based on individual acoustic sources) not shared by equilibrium sensors, and that an evolutionary transition from one sensor type to the other must have involved not simply gaining access to the appropriate stimuli but profound structural changes resulting in a shift in system dynamic order.

Acknowledgement

This work was supported by the National Institute of Deafness and Communicative Disorders (National Institute of Health Grant DC-00112).

References

Anderson, J.H., R.H.I. Blanks, and W. Precht (1978) Response characteristics of semicircular canal and otolith systems in cat. I. Dynamic responses of primary vestibular fibers. Exp. Brain Res., *32:* 491–507.

Baird, R.A., and E.R. Lewis (1986) Correspondences between afferent innervation patterns and response dynamics in the bullfrog utricle and lagena. Brain Research, *369:* 48–64.

Baird, R.A., H. Koyama, E.L. Leverenz, and E.R. Lewis (1980) Functions of otoconial and auditory organs of the bullfrog inner ear identified with intracellular dye. Soc. Neuroscience Abstr., *6:* 223.

Baird, R.A., G. Desmadryl, C. Fernández, and J. Goldberg (1988) The vestibular nerve of the chinchilla II. Relation between afferent response properties and the peripheral innervation patterns in the semicircular canals. J. Neurophysiol., *60* (1): 182–203.

Blanks, R.H.I., and W. Precht (1976) Functional characterization of primary vestibular afferents in the frog. Exp. Brain Res., *25:* 369–390.

Boord, R.L., and G.L. Rasmussen (1963) Projection of the cochlear and lagenar nerves in the cochlear nuclei of the pigeon. J. Comp. Neurol., *120:* 463–475.

Boord, R.L., and H.J. Karten (1974) The distribution of primary lagenar fibers within the vestibular nuclear complex of the pigeon. Brain Behav. Evol., *10:* 228–235.

Brune, J.N., and J. Oliver (1959) The seismic noise of the earth's surface. Bull. Seismolog. Soc. Am., *49* (4): 349–353.

Carney, L.H., and T.C.T. Yin (1988) Temporal coding of resonances by low-frequency auditory nerve fibers: Single-fiber responses and a population model. J. Neurophysiol., *60* (5): 1653–1677.

Caston, J., W. Precht, and R.H.I. Blanks (1977) Response characteristics of frog's lagena afferents to natural stimulation. J. Comp. Physiol., *118:* 273–289.

Cortopassi, K.A., and E.R. Lewis (1996) High-frequency tuning properties of bullfrog lagenar vestibular afferent fibers. J. Vestib. Res., *6* (2): 105–119.

Curthoys, I.S. (1982) The response of primary horizontal semicircular canal neurons in the rat and guinea pig to angular acceleration. Exp. Brain Res., *47* (2): 286–294.

de Boer, E., and P. Kuyper (1968) Triggered correlation. IEEE Trans. Bio-Med. Eng., *BME-15* (3): 169–179.

de Boer, E., and H.R. de Jongh (1978) On cochlear encoding: potentialities and limitations of the reverse-correlation technique. J. Acoust. Soc. Am., *63* (1): 115–135.

de Vries, H.L. (1950) The mechanics of the labyrinth otoliths. Acta Otolaryng. (Stockholm), *38:* 262–273.

Dickman, J.D., and M.J. Correia (1989) Responses of pigeon horizontal semicircular canal afferent fibers. II. High-frequency mechanical stimulation. J. Neurophysiol., *62* (5): 1102–1112.

Didier, A., and Y. Cazals (1989) Acoustic responses recorded from the saccular bundle on the eighth nerve of the guinea pig. Hearing Res., *37:* 23–128.

Dullemeijer, P. (1970) Evolution of patterns and patterns of evolution. forma et functio, *3:* 223–232.

Eggermont, J.J. (1993) Wiener and Volterra analyses applied to the auditory system. Hearing Res., *66:* 177–201.

Evans, E.F. (1988) Cochlear filtering: a view seen through the temporal discharge patterns of single cochlear nerve fibers. *In* Cochlear Mechanics (ed. by W.P. Wilson and D.T. Kemp), Plenum Press, New York, pp. 241–250.

Ezure, K., R.H. Schor, and K. Yoshida (1978) The response of horizontal semicircular canal afferents to sinusoidal rotation in the cat. Exp. Brain Res., *33* (1): 27–39.

Feng, A.S., P.M. Narins, and R.R. Capranica (1975) Three populations of primary auditory fibers in the bullfrog *(Rana catesbeiana)*: their peripheral origins and frequency sensitivities. J. Comp. Physiol., *100:* 221–229.

Fernández, C., and J.M. Goldberg (1971a) Physiology of peripheral neurons innervating semicircular canals of the squirrel monkey. II. Response to sinusoidal stimulation and dynamics of peripheral vestibular system. J. Neurophysiol., *34* (4): 661–675.

Fernández, C., and J.M. Goldberg (1971b) Physiology of peripheral neurons innervating semicircular canals of the squirrel monkey. III. Variations among units in their discharge properties. J. Neurophysiol., *34* (4): 676–681.

Fernández, C., and J.M. Goldberg (1976a) Physiology of peripheral neurons innervating otolith organs of the squirrel monkey. I. Response to static tilts and to long-duration centrifugal force. J. Neurophysiol., *39* (5): 970–984.

Fernández, C., and J.M. Goldberg (1976b) Physiology of peripheral neurons innervating otolith organs of the squirrel monkey. III. Response dynamics. J. Neurophysiol., *39* (5): 996–1008.

Fernández, C., J.M. Goldberg, and W.K. Abend (1972) Response to static tilts of peripheral neurons innervating otolith organs of the squirrel monkey. J. Neurophysiol., *35* (2): 978–997.

Frantti, G.E., D.E. Willis, and J.T. Wilson (1962) The spectrum of seismic noise. Bull. Seismolog. Soc. Am., *52* (1): 113–121.

Furukawa, T., and Y. Ishii (1967) Neurophysiological studies on hearing in goldfish. J. Neurophysiol., *30* (6): 1377–1403.

Goldberg, J.M., G. Desmadryl, R.A. Baird, and C. Fernández (1990) The vestibular nerve of the chinchilla. IV. Discharge properties of utricular afferents. J. Neurophysiol., *63* (4): 781–790.

Hamilton, D.W. (1963) Posterior division of the eighth cranial nerve in *Lacerta vivipara*. Nature (Lond.), *200:* 705–706.

Hartmann, R., and R. Klinke (1980) Discharge properties of afferent fibres of the goldfish semicircular canal with high frequency stimulation. Pflügers Arch., *388:* 111–121.

Hartmann, W.M. (1988) Pitch perception and the segregation and integration of auditory entities. *In* Auditory Function: Neurobiological Bases of Hearing (ed. by G.M. Edelman, W. Einar Gall, and W.M. Cowan), John Wiley & Sons, New York, pp. 623–645.

Hetherington, T.E. (1989) Use of vibratory cues for detection of insect prey by the sandswimming lizard *Scincus scincus.* Animal Behavior, *37:* 290–297.

Koyama, H., E.R. Lewis, E.L. Leverenz, and R.A. Baird (1982) Acute seismic sensitivity in the bullfrog ear. Brain Research, *250:* 168–172.

Lewis, E.R. (1983) Dual acoustical sensitivity in frogs. *In* Hearing – Physiological Bases and Psychophysics (ed. by R. Klinke and R. Hartmann), Springer-Verlag, Berlin, pp. 61–69.

Lewis, E.R. (1988) Tuning in the bullfrog ear. Biophys. J., *53:* 441–447.

Lewis, E.R. (1992) Convergence of design in vertebrate acoustic sensors. *In* The Evolutionary Biology of Hearing (ed. by D.B. Webster, R.R. Fay, and A.N. Popper), Springer-Verlag, New York, pp. 163–184.

Lewis, E.R., and C.W. Li (1975) Hair cell types and distributions in the otolithic and auditory organs of the bullfrog. Brain Research, *83:* 35–50.

Lewis, E.R., and P.M. Narins (1985) Do frogs communicate with seismic signals? Science, *227:* 187–189.

Lewis, E.R., R.A. Baird, E.L. Leverenz, and H. Koyama (1982a) Inner ear: dye injection reveals peripheral origins of specific sensitivities. Science, *215:* 1641–1643.

Lewis, E.R., E.L. Leverenz, and H. Koyama (1982b) The tonotopic organization of the bullfrog amphibian papilla, an auditory organ lacking a basilar membrane. J. Comp. Physiol., *145:* 437–445.

Lewis, E.R., M.G. Sneary, and X. Yu (1990) Further evidence for tuning mechanisms of high dynamic order in lower vertebrates. *In* The Mechanics and Biophysics of Hearing (ed. by P. Dallos, C.D. Geisler, J.W. Matthews, M.A. Ruggero, and C.R. Steele), Lecture Notes in Biomathematics, Vol. 87, Springer-Verlag, New York, pp. 139–146.

Lowenstein, O., and T.D.M. Roberts (1950) The equilibrium function of the otolith organs of the thornback ray *(Raja clavata).* J. Physiol., *110:* 392–415.

Lowenstein, O., and T.D.M. Roberts (1951) The localization and analysis of the responses to vibration from the isolated elasmobranch labyrinth. A contribution to the problem of the evolution of hearing in vertebrates. J. Physiol., *114:* 471–489.

Lowenstein, O., and R.D. Saunders (1975) Otolith-controlled responses from the first-order neurons of the labyrinth of the bullfrog *(Rana catesbeiana)* to changes in linear acceleration. Proc. R. Soc. (Lond.) B, *191:* 475–505.

Mayne, R. (1974) A system concept of the vestibular organs. *In* Handbook of Sensory Physiology, Vol 6 Part 2 (ed. by H.H. Kornhuber), Springer-Verlag, New York, pp. 493–580.
McCue, M.P., and J.J. Guinan (1993) Acoustic responses from primary afferent neurons of the mammalian sacculus. Assoc. Res. Otolaryngol. Abstr., *16:* 33.
McCue, M.P., and J.J. Guinan (1994) Acoustically responsive fibers in the vestibular nerve of the cat. J. Neurosci., *14* (10): 6058–6070.
Møller, A.R. (1977) Frequency selectivity of single auditory-nerve fibers in response to broadband noise stimuli. J Acoustic. Soc. Am., *62* (1): 135–142.
Myers, S.F., and E.R. Lewis (1991) Vestibular afferent responses to microrotational stimuli. Brain Research, *543:* 36–44.
Narins, P.M. (1975) Electrophysiological determination of the function of the lagena in terrestrial amphibians. Biological Bulletin, *149* (2): 438.
Oeckinghaus, H. (1985) Modulation of activity in starling cochlear ganglion units by middle-ear muscle contractions, perilymph movements and lagena stimuli. J. Comp. Physiol. A Sen. Neur. Behav. Physiol., *157* (5): 643–655.
O'Leary, D.P., and V. Honrubia (1976) Analysis of afferent responses from isolated semicircular canal of the guitarfish using rotational acceleration white-noise inputs. II. Estimation of linear system parameters and gain and phase spectra. J. Neurophysiol., *39* (3): 645–659.
Platt, C. (1973) Central control of postural orientation in flatfish I. Postural change dependence on central neural changes. J. Exp. Biol., *59:* 491–521.
Platt, C. (1983) The peripheral vestibular system of fishes. *In* Fish Neurobiology. Vol. 1. Brain Stem and Sensory Organs (ed. by R.G. Northcutt and R.E. Davis), University of Michigan Press, Ann Arbor, pp. 89–123.
Platt, C., and A.N. Popper (1981) Fine structure and function of the ear. *In* Hearing and Sound Communication in Fishes (ed. by W.N. Tavolga, A.N. Popper, and R.R. Fay), Springer-Verlag, New York, pp. 3–38.
Sneary, M.G., and E.R. Lewis (1989) Response properties of turtle auditory afferent nerve fibers: evidence for a high order tuning mechanism. *In* Cochlear Mechanisms (ed. by J.P. Wilson and D.T. Kemp), Plenum Publishing Corp., New York, pp. 235–240.
Steinhausen, W. (1931) Über den Nachweis der Bewegung der Cupula in der intakten Bogengangsampulle des Labyrinths bei der natürlichen rotatorischen und calorischen Reizung. Pflügers Arch. gesamte Physiol., *228:* 322–328.
Steinhausen, W. (1933) Über die Beobachtung der Cupula in der Bogengangsampulle des Labyrinthes des lebenden Hechts. Pflügers Arch. gesamte Physiol., *232:* 500–512.
Stewart, W.W. (1978) Functional connections between cells as revealed by dye-coupling with a highly fluorescent naphthalimide tracer. Cell, *14:* 741–759.
Thorson, J., and M. Biederman-Thorson (1974) Distributed relaxation processes in sensory adaptation. Science, *183:* 161–172.
van Egmond, A.A.J., J.J. Groen, and L.B.W. Jongkees (1949) The mechanics of the semicircular canal. J. Physiol. (Lond.), *110:* 1–17.
von Frisch, K. (1938) Über die Bedeutung des Sacculus und der Lagena für den Gehörsinn der Fische. Z. Vergl. Physiologie, *25:* 703–747.
Walkowiak, W., and H. Münz (1985) The significance of water surface-waves in the communication of fire-bellied toads. Naturwissenschaften, *72:* 49–51.
Wever, E.G. (1974) The Evolution of vertebrate hearing. *In* Handbook of Sensory Physiology, Vol. V/1. Auditory System. Anatomy and Physiology (Ear) (ed. by W.D. Keidel and W.D. Neff), Springer-Verlag, Berlin, pp. 423–454.
Wilson, V.J., and G. Melvill Jones (1979) Mammalian Vestibular Physiology. Plenum Press, New York, pp. 41–76.
Wit, H.P., J.D. Bleeker, and H.H. Mulder (1984) Responses of pigeon vestibular nerve fibers to sound and vibration with audiofrequencies. J. Acoust. Soc. Am., *75* (1): 202–208.
Yost, W.A. (1991) Auditory image perception and analysis: the basis for hearing. Hearing Res., *56:* 8–18.
Young, E.D., C. Fernández, and J.M. Goldberg (1976) Sensitivity of vestibular nerve fibers to audiofrequency sound and head vibration in the squirrel monkey. J. Acoust. Soc. Am., *59* (1): S47.
Young, E.D., C. Fernández, and J.M. Goldberg (1977) Responses of squirrel monkey vestibular neurons to audio-frequency sound and head vibration. Acta Otolaryngol., *84:* 351–360.
Yu, X., E.R. Lewis, and D. Feld (1991) Seismic and auditory tuning curves from bullfrog saccular and amphibian papillar axons. J. Comp. Physiol. A, *169:* 241–248.